

Electronic Supplementary Information (ESI)

**Investigation of continuous changes of electric-field-induced electronic  
state in  $\text{Bi}_{1-x}\text{Ca}_x\text{FeO}_{3-\delta}$**

Atsushi Ikeda-Ohno,<sup>1,2</sup> Ji Soo Lim,<sup>3</sup> Takuo Ohkochi,<sup>4</sup> Chan-Ho Yang<sup>3,5</sup> and Jan Seidel<sup>6\*</sup>

<sup>1</sup> *School of Civil and Environmental Engineering, The University of New South Wales  
(UNSW), Sydney, NSW 2052, Australia*

<sup>2</sup> *Institute for Environmental Research, Australian Nuclear Science and Technology  
Organisation (ANSTO), Locked Bag 2001, Kirrawee DC, NSW 2232, Australia*

<sup>3</sup> *Department of Physics, Korea Advanced Institute of Science and Technology (KAIST),  
Daejeon 305-701, Republic of Korea*

<sup>4</sup> *Japan Synchrotron Radiation Research Institute (JASRI), SPring-8, Sayo-cho, Hyogo 679-  
5198, Japan*

<sup>5</sup> *Institute for the NanoCentury, Korea Advanced Institute of Science and Technology (KAIST),  
Daejeon 305-701, Republic of Korea*

<sup>6</sup> *School of Materials Science and Engineering, The University of New South Wales (UNSW),  
Sydney, NSW 2052, Australia*

(\*E-mail: [jan.seidel@unsw.edu.au](mailto:jan.seidel@unsw.edu.au))

## Experimental details

**Sample growth.** BiFeO<sub>3</sub> thin films doped with 10, 20, 30, and 40% Ca were grown on (001) SrTiO<sub>3</sub> substrates using pulsed laser deposition (PLD) at 675 °C in 30 Torr oxygen pressure. A 2 nm thick LaAlO<sub>3</sub> capping layer was deposited *in-situ* as an oxygen barrier on top of the Ca-doped BiFeO<sub>3</sub> layers to prevent oxygen loss during electrical poling. Standard lift-off lithography was used to produce Pt electrode patterns with a separation of 20 microns on top of the thin films for local electrical poling experiments. Ar ion milling was also employed to remove the capping layer between the film and the Pt electrode. Typical PLD deposition rates were ~3 nm/min at a laser repetition rate of 10 Hz. The pulsed KrF excimer laser with a wavelength of 248 nm was focused to reach a laser fluence of ~1 J/cm<sup>2</sup> on the target surface. The films were cooled down at a rate of 10 °C/min in 500 Torr oxygen pressure. The thicknesses of Ca-doped BiFeO<sub>3</sub> layers were approximately 100 nm.

**XRD and electrical poling.** Ca-substitution of the material under investigation leads to the formation of compensating oxygen vacancies.<sup>1-3</sup> The crystal structure details of the Ca doped materials as compared to the undoped material were determined by X-ray diffraction  $\theta$ - $2\theta$  scans (Panalytical X'Pert MRD Pro) with Cu K $\alpha$  radiation (see Fig. S1). In order to make non-equilibrium but long-lasting oxygen vacancy deficient/rich states locally, an electric voltage of 15 V was applied across a pair of Pt electrodes<sup>i</sup> for an hour at 250 °C in air. After the electric forming, films were suddenly cooled to room temperature to prevent diffusion of oxygen vacancies. Another pair of Pt electrodes on the same film was prepared to define a reference region not being exposed to electric voltage for comparison. The electrically-formed region showed dark contrast observed through a typical optical microscope. In order to remove charging effects during PEEM measurements, a very thin Au layer (~2 nm thickness) was deposited on the exterior areas of the poled and unpoled regions.

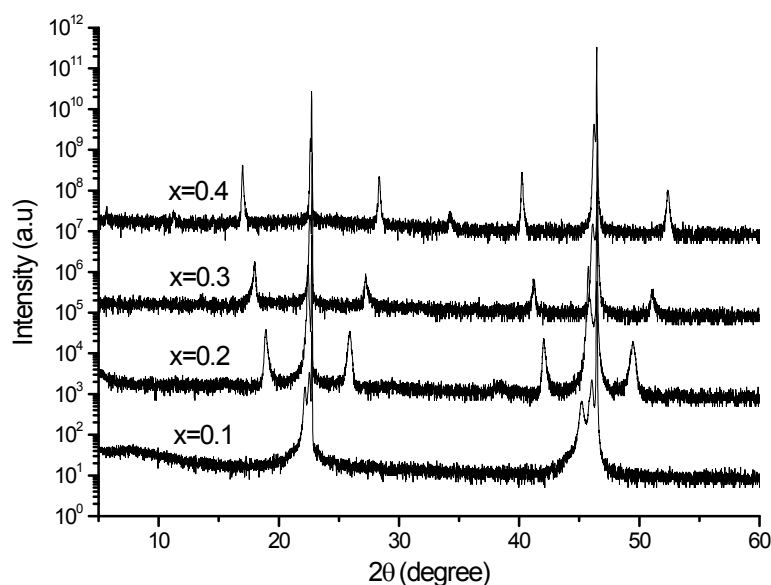


**Fig. S1.** X-ray diffraction patterns ( $\theta$ - $2\theta$  scans) of Bi<sub>1-x</sub>Ca<sub>x</sub>FeO<sub>3-δ</sub> films on SrTiO<sub>3</sub> for selected Ca substitution levels at room temperature. The films show superstructure peaks due to oxygen vacancy ordering.

**PEEM experiments.** Photoelectron emission microscopy (PEEM) images were collected at the beamline BL25SU,<sup>4</sup> SPring-8, using a valid-line-spacing plane grating (VLSPG) with a compact PEEM apparatus (PEEMSPECTOR, Elmitec GmbH).<sup>5</sup> The samples were mounted on a sample stage installed in a vacuum chamber ( $\sim 7 \times 10^{-8}$  Pa). All measurements were performed at room temperature. The energy calibration of the VLSPG monochromator was carried out at Ca L<sub>II,III</sub>-edges (CaCO<sub>3</sub>) and at Fe L<sub>III</sub>-edge (Sr<sub>3</sub>Fe<sub>5</sub>O<sub>12</sub>).

**XAS spectra acquisition from PEEM images.** A series of the PEEM images acquired at different incident X-ray energies was loaded on Igor Pro (Version 6.0) with the dedicated program suite SPELEEM developed by Andrea Locatelli at Elettra.<sup>6</sup> Drifting of the acquired images was corrected by using a correction macro on SPELEEM. For acquiring O K-edge and Fe L<sub>II,III</sub>-edge XAS data from the PEEM images, the area between the two electrodes was divided into seven isometric sub-areas having 1.56  $\mu\text{m}$ -width relative to the horizontal of the acquired PEEM image (Regions of interest, ROI, see Fig. 3-(a) and Fig. S2-(a)) and two additional ROIs were defined on the left- and right electrode areas, where the photoelectric effects associated with oxygen and iron atoms are negligible. In case of O K-edge XAS, the ROI which is the most adjacent to the left electrode area (ROI 1 (blue) in Fig. 3-(a)) was further divided into five sub-areas to obtain the XAS spectra with finer spatial resolution. On the defined nine ROIs, the emission spectra were created by SPELEEM macros. In order to convert the obtained emission spectra into X-ray absorption spectra, the emission intensity must be normalised with the incident X-ray intensity. It is practically impossible to directly measure the intensity of the incident X-rays irradiated on each ROI area. Therefore, the intensity of incident X-rays on the ROI area between the electrodes was estimated by the linear combination of the emission intensity of the left- and right electrode areas, based on the distances of each ROI centre from the two electrodes. This also corrects the spatial variation of incident X-ray intensity at different ROI areas. The obtained O K-edge XAS data was further normalised at 555 eV where oxygen 1s XAS exhibit no spectral feature depending on the Ca-doping level,<sup>ii</sup> whilst the Fe L<sub>II,III</sub>-edge XAS data was normalised at 730 eV where no doping-dependent spectral feature is observed. The incident X-rays employed in the present PEEM experiments have energy gradation only in the horizontal direction (approximately 0.5 eV / 100  $\mu\text{m}$  in the longitudinal direction of Fig. 3-(a)). Therefore, performing ROI scans in the lateral direction of Fig. 3-(a) are not influenced by the energy gradation of incident X-rays.

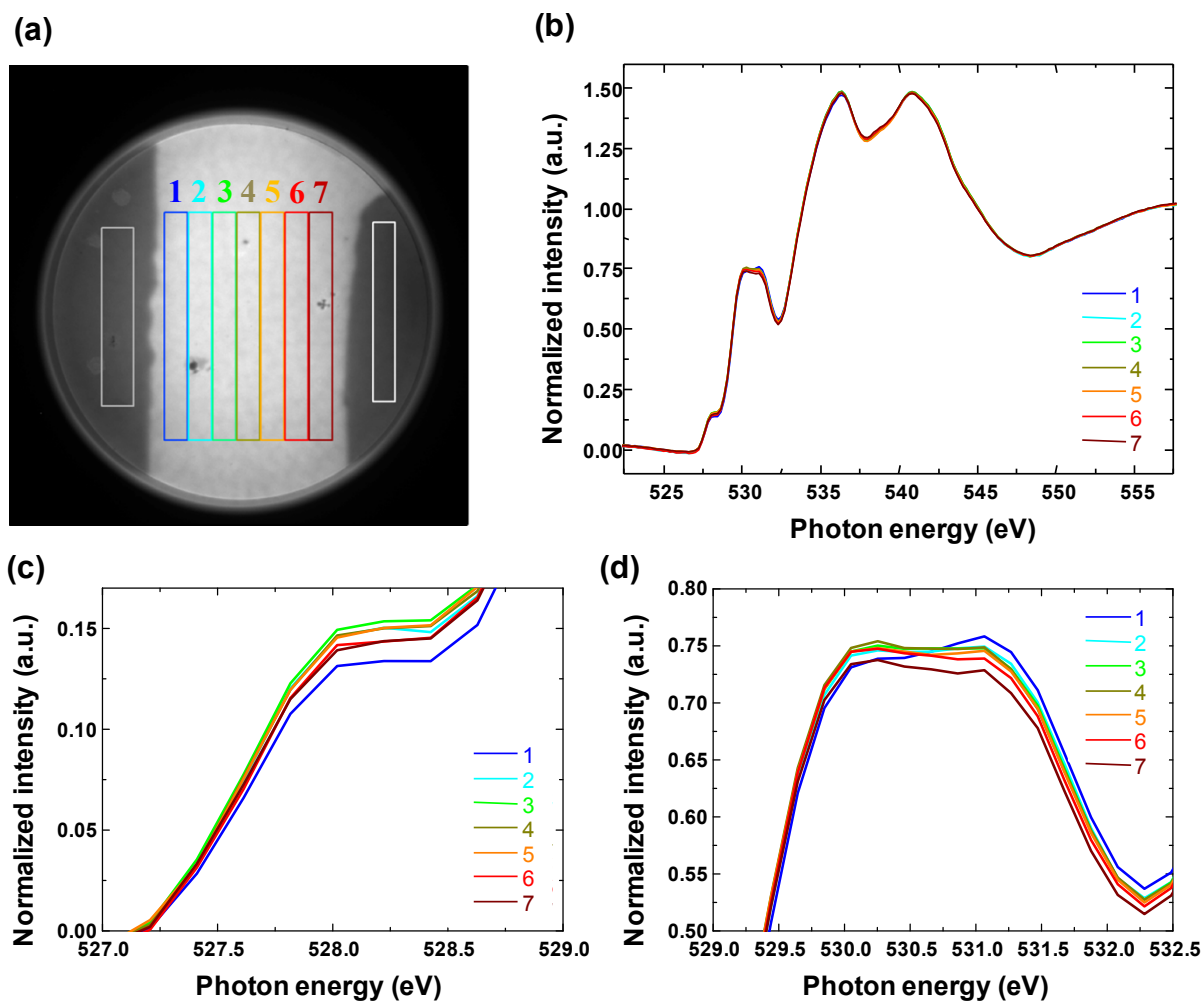


**Fig. S2.** (a) PEEM image of 30%-Ca substitution sample at 530.0 eV. Dark areas within circle are Pt electrodes used for electrical poling (electrode gap is 20 microns). Regions of interest (ROI) for acquiring local XAS spectra between electrodes are numbered from 1 to 7. (b) O K-edge XANES spectra of 30%-Ca substitution sample at different ROI areas in (a). (c-d) Enlargement of O K-edge XANES spectra in (b): (c) region from 527.0 to 529.0 eV, (d) region from 529.0 to 532.5 eV. (The right-side electrode was biased with a positive voltage of 15 V during the electric forming process.)

**Peak deconvolution analysis on O-XAS spectra.** Fitting parameters of peak deconvolution analysis for O-XAS spectra in Fig. 1 are summarised in the following table.

Sample	Peak 1			Peak 2			Peak 3			
	Position / eV	Height	FWHM	Position / eV	Height	FWHM	Position / eV	Height	FWHM	
10%-Ca	Poled	528.1759606	0.067943	1.182566	529.7539481	0.603721	1.02065	531.1681524	0.886734	1.468012
	Unpoled	528.3617561	0.024302	1.370895	529.7762855	0.634981	0.991578	531.2135408	1.058058	1.610547
20%-Ca	Poled	528.1529139	0.120265	1.111978	529.682976	0.55887	1.136216	531.1522107	0.851026	1.633784
	Unpoled	528.4047025	0.011965	0.469193	529.7035873	0.551659	1.040712	531.1525153	0.966774	1.740866
30%-Ca	Poled	528.0503718	0.165483	1.025496	529.8657371	0.625527	1.487341	531.2168916	0.539608	1.419129
	Unpoled	528.2137288	0.016836	1.300506	529.9125444	0.625219	1.333721	531.1788141	0.513775	1.468978
40%-Ca	Poled	527.9659017	0.342262	0.996902	529.7855251	0.512638	2.096016	531.2741602	0.387896	1.305934
	Unpoled	528.214541	0.052602	1.087203	529.7990291	0.524493	1.197745	531.1028625	0.55103	1.485504

---

## References

1. C.-H. Yang, J. Seidel, S. Y. Kim, *et al.*, *Nature Mater.*, 2009, **8**, 485.
2. J. Seidel, W. Luo, S. J. Suresha, *et al.*, *Nature Comm.*, 2011, **3**, 799.
3. J. Schiemer, R. Withers, L. Noren, *et al.*, *Chem. Mater.*, 2009, **21**, 4223.
4. T. Muro, T. Nakamura, T. Matsushita, T. Wakita, K. Fukumoto, H. Kimura, T. Hirano, T. Kinoshita, T. Hara, K. Shirasawa, M. Takeuchi, H. Kitamura, *AIP Conf. Proc.*, 2007, **879**, 571.
5. K. Arai, T. Okuda, A. Tanaka, K. Fukumoto, T. Hasegawa, T. Nakamura, T. Matsushita, T. Muro, A. Kakizaki, T. Kinoshita, *J. Appl. Phys.*, 2001, **110**, 084306.
6. <http://www.elettra.trieste.it/PEOPLE/index.php?n=AndreaLocatelli.DataAnalysis>.